Available online www.worldscientificnews.com

World Scientific News

An International Scientific Journal

WSN 208 (2025) 106-125 EISSN 2392-2192

Crystal Structure, Hirshfeld Surface Analysis, and Computational Study of (*E*)-2-Phenyl-*N*'-(1,7,7-Trimethylbicyclo[2.2.1]Heptan-2-Ylidene)Acetohydrazide

Mukesh B. Parmar[1,2], Jignesh H. Pandya[1] *, Manisha K. Vara[2]

[2]Department of Chemistry, H. & H. B. Kotak Institute of Science, Rajkot – 360001, India

[2]Envitro Laboratories Private Limited, Envitro Group of Companies, Rajkot, Gujarat-360004, India

*E-mail address: jhpandya@gmail.com (Dr. J. H. Pandya)

ABSTRACT

The crystal structure of camphor derived Schiff base (*E*)-2-phenyl-*N*'-(1,7,7-trimethylbicyclo[2.2.1]heptan-2-ylidene)acetohydrazide ($C_{18}H_{24}N_2O$), was determined by single-crystal X-ray diffraction. The compound crystallizes in the orthorhombic space group $Pna2_1$, with unit cell parameters a = 8.2157(5) Å, b = 15.6570(13) Å, c = 12.5573(10) Å, and Z = 4. The molecule adopts an *E*-configuration across the imine bond, and the rigid bicyclic camphor scaffold enforces structural stability. Hirshfeld surface analysis revealed dominant H···H and C···H/H···C interactions, supported by 2D fingerprint plots. The energy framework and interaction energy calculations using B3LYP/6-31G(d,p) level theory confirmed dispersion as the principal stabilizing force in the crystal packing, with the strongest intermolecular interaction recorded at −72.4 kJ/mol. The structure was refined to R_1 = 0.0582 and wR_2 = 0.1454 for [I > 2σ(I)], with an absolute structure parameter of −0.4(5). These findings provide insights into the supramolecular architecture of camphor-based Schiff bases and underscore their potential applications in medicinal chemistry.

***Keywords*:** Crystal structure, Hirshfeld surface analysis, Schiff base, camphor.

(Received 22 August 2025; Accepted 18 September 2025; Date of Publication 6 October 2025)

1. CHEMICAL CONTEXT

Camphor is a plant-derived monoterpenoid that can be isolated in chemically pure form. **Figure 1** shows the molecular structure showing atom labeling of scheme and displacement ellipsoids at the 50% probability level. Schiff bases have various applications in medicinal chemistry, and in our study, they served as a key motivation for structural investigation. The titled compound found active against MCF-7 cell line.

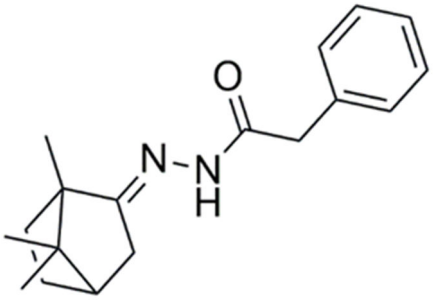

Figure 1. (*E*)-2-phenyl-*N*'-(1,7,7-trimethylbicyclo[2.2.1]heptan-2-ylidene)acetohydrazide.

As part of complementary structural studies on this molecules, the crystal and molecular structure is described herein, detailed analysis of the calculated Hirshfeld surfaces. Synthesis procedure of MBL-101, (*E*)-2-phenyl-*N*'-(1,7,7-trimethylbicyclo[2.2.1]heptan-2-ylidene)acetohydrazide, was reported by *M. K. Vara* et al. [1]. Crystals in the form of light yellow blocks for the X-ray study were grown by the slow evaporation of its chloroform solution.

2. STRUCTURAL COMMENTARY

Crystal data, data collection, and structure refinement details are summarized in **Table 1** and **Table 2**. The titled Schiff base MBL-101, shows the molecular structure showing atom-labeling of scheme and displacement ellipsoids at the 50% probability level in **Figure 2**, features one imine bond, C9=N1 [1.269 (4) Å] with configuration being *E*. **Table 3** providing an indication of atomic thermal motion. Among the carbon atoms, C(1) is located at coordinates (5295, 994, 2630) with a U(eq) of 48. C(2) and C(3) follow with coordinates (5111, 1021, 1545) and (5823, 1677, 964), and displacement parameters of 66 and 70, respectively. Notably, C(4) shows a higher U(eq) of 77, suggesting increased thermal motion at (6708, 2268, 1471). Carbon atoms C(5) through C(18) exhibit a range of displacement parameters from 34 to 90, with C(17) having the highest value, possibly indicating greater dynamic disorder or flexibility at this position.

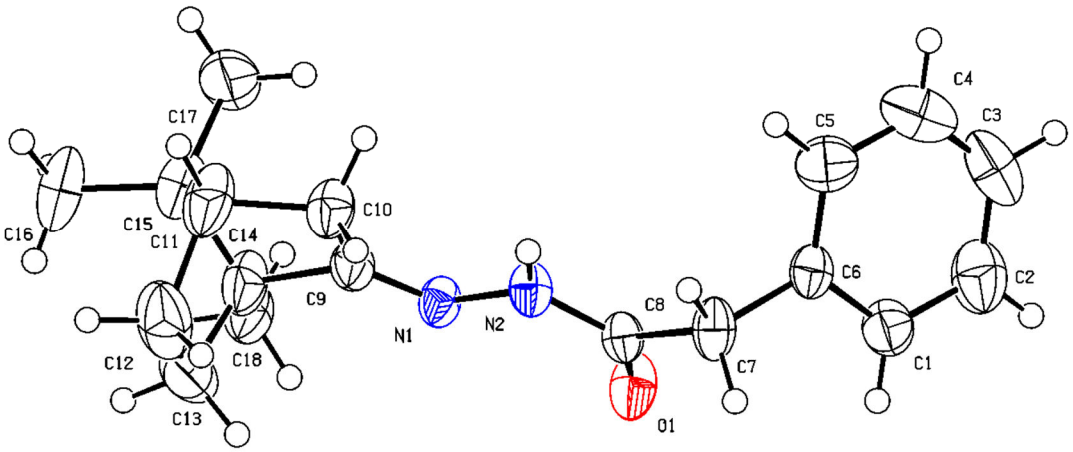

Figure 2. The molecular structure (MBL-101) showing atom-labeling of scheme and displacement ellipsoids at the 50% probability level.

For nitrogen atoms, N(1) and N(2) are located at (4483, 2955, 6293) and (5611, 2598, 5604), respectively, both with relatively low and stable U(eq) values of 34. The oxygen atom O(1), situated at (3747, 1687, 4923), shows a slightly higher displacement parameter of 49, consistent with the generally higher mobility often observed for oxygen atoms in such molecular frameworks. These atomic coordinates and thermal parameters provide essential information for the precise structural modeling of MBL-101. **Table 4** providing a comprehensive view of the molecular geometry. The molecule exhibits standard aromatic and aliphatic carbon-carbon bond lengths. For example, the C(1)–C(2) and C(1)–C(6) bonds measure 1.372 Å and 1.381 Å, respectively, while C(2)–C(3) and C(3)–C(4) are slightly shorter at 1.389 Å and 1.337 Å, indicating aromatic character. The aliphatic bond C(6)–C(7) is longer, at 1.508 Å, consistent with single-bond geometry. The C(7)–C(8) and C(10)–C(11) bonds are also within the range for saturated carbon chains, measuring 1.517 Å.

Heteroatom bond lengths include C(8)–O(1) at 1.219 Å and C(8)–N(2) at 1.342 Å, indicating the presence of a carbonyl and amine group. Additionally, the N(1)–N(2) bond is 1.385 Å, which is typical for a single N–N linkage. Bond angles around sp^2 hybridized centers like C(2)–C(1)–C(6) (120.7°) and C(3)–C(2)–C(1) (119.8°) confirm the planar geometry of the aromatic ring. Hydrogen bonding geometries and tetrahedral angles are observed throughout the saturated carbon atoms. For instance, C(7)–H(7A) and C(7)–H(7B) each measure 0.970 Å, with bond angles such as H(7A)–C(7)–H(7B) close to the ideal tetrahedral angle (107.8°). The angles around methylene and methyl groups (e.g., C(15)–C(16)–H(16A) at 109.5° and C(13)–C(14)–C(9) at 116.0°) also support this. Key angular interactions involving heteroatoms include O(1)–C(8)–N(2) at 123.9°, O(1)–C(8)–C(7) at 121.5°, and N(2)–C(8)–C(7) at 114.6°, reflecting electron delocalization and sp^2 hybridization around the carbonyl group. The N(1)–C(9)–C(10) angle is wider (130.5°), possibly due to steric strain or lone pair repulsion from adjacent atoms.

Overall, the structural parameters confirm a well-defined molecular framework with consistent geometry across aromatic, aliphatic, and heteroatomic regions, indicating good molecular stability and symmetry in MBL-101. **Table 5** describes the thermal motion of atoms in three-dimensional space, modeled as ellipsoids. In MBL-101, most carbon atoms exhibit moderate anisotropy. For instance, C(1) has U values of U11=47, U22=53, and U33=44, with minor off-diagonal terms, suggesting relatively isotropic thermal motion. However, atoms like C(3) and C(4) show significantly larger anisotropy, with C(3) having a particularly high U22=108, indicating increased vibrational freedom along one axis. C(17) exhibits extreme anisotropy, especially in U11=164, which may point to dynamic disorder or high flexibility in this part of the molecule. Nitrogen atoms N(1) and N(2) display relatively small and balanced displacement parameters, such as N(1) with U11=28, U22=37, and U33=38, reflecting limited motion and a well-ordered environment. Oxygen atom O(1) shows moderate anisotropy with U22=63 and a notable negative cross-term U23=−23, indicating directional thermal movement.

The ADPs suggest that while most atoms in MBL-101 occupy well-defined positions with constrained thermal motion, a few atoms—particularly in aliphatic or peripheral positions—exhibit enhanced flexibility, consistent with the molecular structure and potential dynamic behavior. **Table 6** values indicate the spatial positions and thermal motion of each hydrogen atom within the crystal structure. Hydrogen atoms bonded to the aromatic and aliphatic carbon framework exhibit a range of thermal vibrations. H(1), positioned at (4787, 565, 3020), has a moderate U(eq) of 58, while H(2) and H(3) show higher values of 79 and 84, respectively, suggesting greater thermal motion. Notably, H(4) and H(5), at (7188, 2705, 1079) and (7544, 2664, 2903), have elevated displacement parameters (92 and 70), indicating significant flexibility in these positions.

Hydrogen atoms on methyl and methylene groups generally display higher U(eq) values due to increased rotational freedom. For example, H(16A), H(16B), and H(16C) each exhibit a high U(eq) of 110, while H(17A), H(17B), and H(17C) show the highest displacement values in the molecule at 134, reflecting pronounced dynamic behavior. In contrast, atoms such as H(7A) and H(7B), located on the central aliphatic chain, exhibit lower U(eq) values of 51, suggesting more restricted motion. The terminal hydrogen atoms of the molecule, including H(18A–C) at coordinates such as (1890, 4117, 7037), all have identical U(eq) values of 77, pointing to moderately flexible terminal group behavior. Additionally, H(2A), associated with the nitrogen atom N(2), shows a notably low U(eq) of 41, consistent with its involvement in stronger bonding or possible hydrogen bonding interactions.

The hydrogen coordinate and displacement data support a well-resolved structure with expected dynamic behavior in flexible side chains and terminal groups, while core hydrogen atoms remain more rigidly defined. **Table 7** presents the torsion angles, provide insight into the molecule's three-dimensional conformation and flexibility. In the aromatic and conjugated systems, torsion angles are generally close to 0° or 180°, reflecting a planar configuration. For example, the sequence C(6)–C(1)–C(2)–C(3) has a torsion angle of –2.2°, and C(1)–C(2)–C(3)–C(4) is 1.3°, indicating near planarity. Similarly, C(2)–C(3)–C(4)–C(5) and C(3)–C(4)–C(5)–C(6) show small torsion angles of –0.3° and 0.3°, respectively, further supporting a flat aromatic ring system. Significant deviations appear in the aliphatic chains and side groups. For example, the angle C(5)–C(6)–C(7)–C(8) is 96.1°, and C(1)–C(6)–C(7)–C(8) is –85.0°, indicating a twisted geometry at this region. Similarly, the torsion angle between C(6)–C(7)–C(8)–O(1) is 61.4°, while that between C(6)–C(7)–C(8)–N(2) is –120.0°, reflecting the non-coplanarity of the substituents on C(8).

Notable torsion angles involving the nitrogen atoms and their connections include N(1)–C(9)–C(10)–C(11) at –174.2°, indicating near-planarity in this linkage, while the C(10)–C(9)–C(14)–C(18) angle is 164.4°, also suggesting a relatively extended conformation. Meanwhile, the O(1)–C(8)–N(2)–N(1) and C(7)–C(8)–N(2)–N(1) angles are 4.7° and –173.9°, respectively, implying slight torsion at the amide region. Angles involving terminal groups and alkyl chains such as C(10)–C(11)–C(15)–C(17) at –62.6°, and C(18)–C(14)–C(15)–C(17) at –64.7°, point to flexible, non-planar side chains. Furthermore, N(1)–C(9)–C(14)–C(15) at –153.2°, and C(13)–C(14)–C(15)–C(17) at 170.8°, indicate varying degrees of twist and conformational strain. Overall, the torsion angles suggest that while the core aromatic ring maintains a planar geometry, the attached side chains and heteroatom-containing regions adopt diverse conformations, contributing to the molecule's three-dimensional shape and potential intermolecular interaction behavior.

3. HIRSHFELD SURFACE ANALYSIS

Crystal Explorer 17.5 was used to generate all surfaces, two-dimensional fingerprint plots, intermolecular interaction, and energy frameworks [2]. The mappings of d_i, d_e, d_{norm}, shape-index and curvedness for the title structure MBL-101 are shown in **Figure 3**. Hirshfeld Surface property is tabulated in **Table 8 to Table 10**.

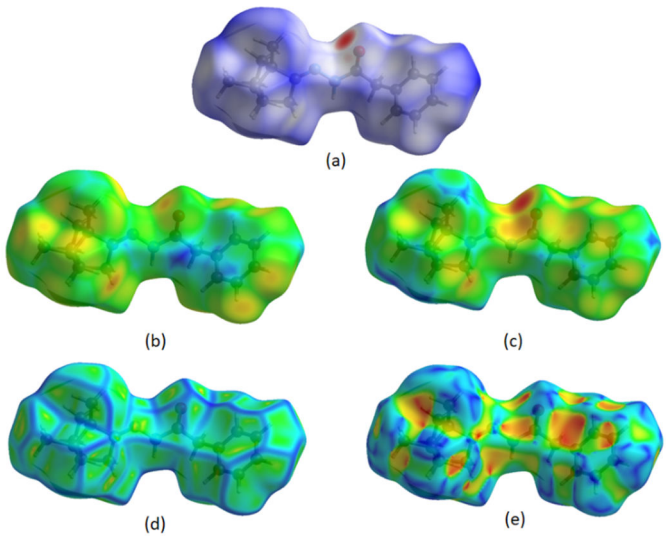

Figure 3. The Hirshfeld surface of MBL-101 mapped with (a) d_{norm}, (b) d_i, (c) d_e, (d) curvedness, and (e) shape-index.

The Hirshfeld surface analysis was performed using high (standard) resolution at an isovalue of 0.5. The calculated molecular volume is 396.54 Å^3, while the surface area measures 354.29 Å^2. The globularity value is 0.737, indicating a fairly compact shape, and the asphericity is 0.302, suggesting a moderate deviation from perfect sphericity. The internal distance (d_i) ranges from a minimum of 0.820 Å to a maximum of 2.557 Å, with a mean value of 1.634 Å. The external distance (d_e) spans from 0.821 Å to 2.458 Å, with an average of 1.650 Å.

The normalized contact distance (d_{norm}) varies between -0.484 and 1.527, with a mean of 0.579. For the shape index, values range from -0.995 to 0.998, with a mean of 0.244, indicating both concave and convex regions on the molecular surface. Curvedness exhibits a wider range, from -3.970 to 0.325, and a mean value of -0.957, reflecting the degree of surface curvature and variation across the molecule.

For the internal distance (d_i), the mean positive value is 1.63 with a Pi value (Asymmetry index) of 0.219 and a SigmaT (total standard deviation -Overall surface diversity) of approximately 2.94×10^{14}, while the Nu value (skewness) is 0. The external distance (d_e) has a mean positive value of 1.65, a Pi value of 0.222, and a SigmaT of about 3.00×10^{14}, with a Nu value also equal to 0. The normalized contact distance (d_{norm}) has a mean positive value of 0.592 and a mean negative value of -0.176, with Pi at 0.226, $Sigma^+$ (Standard deviation of positive value) at 7.76×10^{8}, $Sigma^-$ (Standard deviation of negative value) at 2.08×10^{4}, and a total sigma of 3.66×10^{13}. Its Nu value is 4.64×10^{-7}. For the shape index, the mean positive and negative values are 0.554 and -0.459, respectively, with Pi at 0.448. The $Sigma^+$ and $Sigma^-$ are 3.39×10^{8} and 4.51×10^{7}, respectively, while SigmaT is 1.19×10^{13}, and Nu is 0.0523. Lastly, the curvedness shows a mean positive value of 0.0648 and a mean negative value of -0.968, with Pi at 0.426. The corresponding $Sigma^+$ is 981, $Sigma^-$ is 2.11×10^{9}, and the total sigma reaches 9.99×10^{13}, with a Nu value of 4.75×10^{-9}.

The d_{norm}-mapped Hirshfeld surface of MBL-101 highlighting diminutive red spots indicates the close contact between the neighbouring molecules near the O1 attached to C8 and H attached to N2 atoms showing close contacts between O1•••H is presented in **Figure 4** and intermolecular hydrogen bond between O1•••HN2, O1•••HC7, C1•••HC11 in unit cell is presented in **Figure 5**. The two-dimensional fingerprint plots provide the close contact of respective elements, as shown in **Figure 6**.

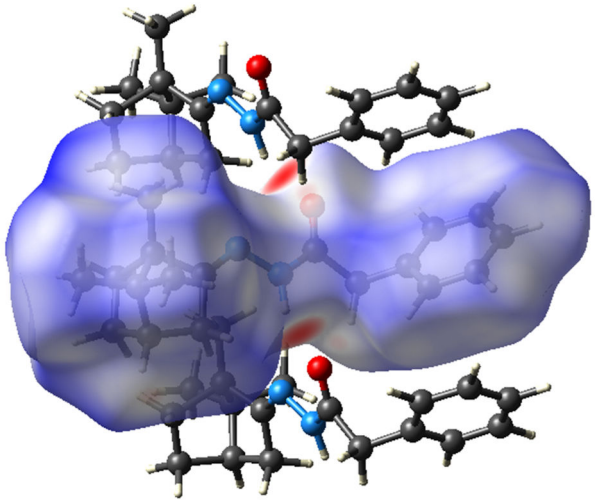

Figure 4. A view of the d_{norm}-mapped Hirshfeld surface for MBL-101 highlighting diminutive red spots near the O1 attached to C8 and H attached to N2 atoms, owing to their participation in O1•••H contacts, showing the intermolecular interactions.

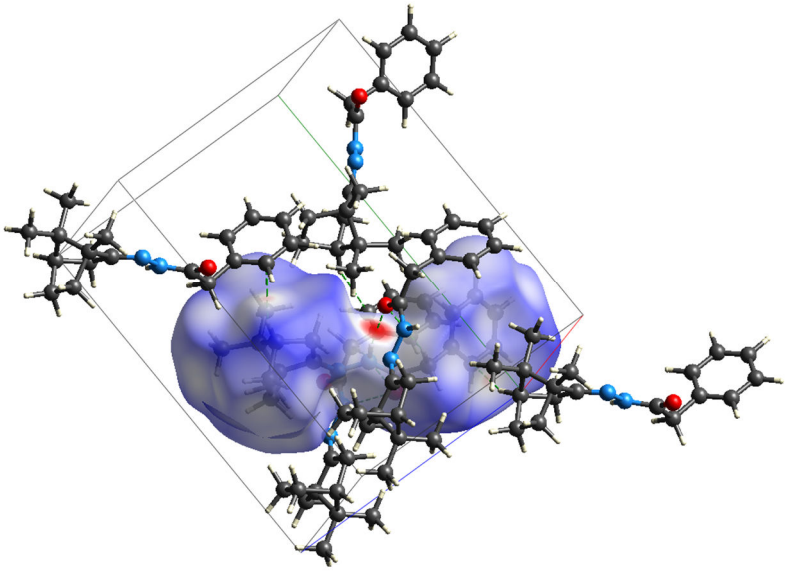

Figure 5. A view of the d_{norm}-mapped Hirshfeld surface for MBL-101 in unit cell, highlighting intermolecular hydrogen bond between O1•••HN2, O1•••HC7, C1•••HC11.

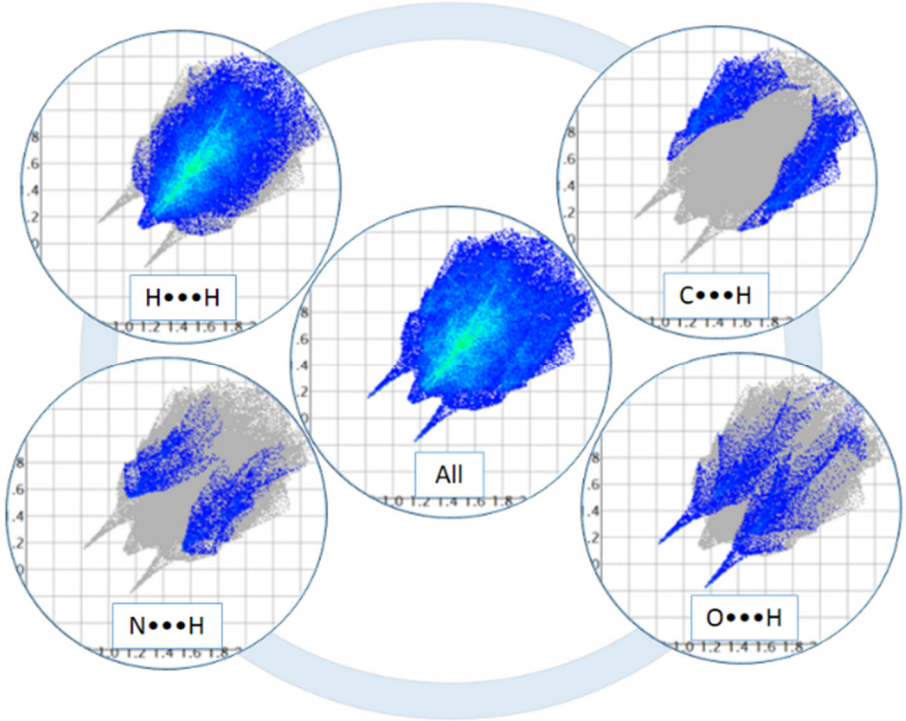

Figure 6. A comparison of the full two-dimensional fingerprint plot (a) for MBL-101 and those delineated into (b) H•••H, (c) C•••H/H•••C, (d) N•••H/H•••N, (e) O•••H/H•••O contacts.

The full two-dimensional fingerprint plot for MBL-101, **Figure 6 (a)**, and those decomposed into H•••H, C•••H/H•••C, N•••H/ H•••N, C•••C and O•••H/H•••O contacts are shown in **Figure 6 (b)-(e)**, respectively. The percentage contributions from the different interatomic contacts to the Hirshfeld surface are quantitatively summarized in **Table 11**, provides insight into atomic interactions across the molecular surface, distinguishing between atoms located on the inside and outside of contacts. Carbon (C) atoms on the outside interact exclusively with hydrogen (H) atoms, contributing 7.9% to the overall fingerprint, while hydrogen atoms show the most extensive interactions. Specifically, hydrogen contributes 6.2% from the inside and interacts externally with carbon (69.2%), nitrogen (3.0%), and oxygen (4.7%), totaling 83.1%. Nitrogen (N) and oxygen (O) atoms are only involved externally, contributing 3.6% and 5.3%, respectively. In total, the inside contributions amount to 6.2%, while outside interactions are dominated by hydrogen at 86.1%, with smaller contributions from nitrogen and oxygen, highlighting hydrogen's central role in intermolecular contacts. Surface area included (as percentage of the total surface area) for close contacts between atoms inside and outside the surface [3, 4].

4. COMPUTATIONAL CHEMISTY

The magnitudes of intermolecular energies were represented graphically in **Figure 7** by energy frameworks whereby the cylinders join the centroids of molecular pairs using a red, green, and blue color scheme for the E_{ele}, E_{disp} and E_{tot} components, respectively; the radius of the cylinder is proportional to the magnitude of interaction energy. The supramolecular architecture in the crystal is significantly influenced by the green cylinders that connect the centroids of molecular pairs, emphasising the dispersion components. Interaction energy details for MBL-101 are providede in the **Table 12** and scale factors for benchmarked energy models is given in **Table 13**.

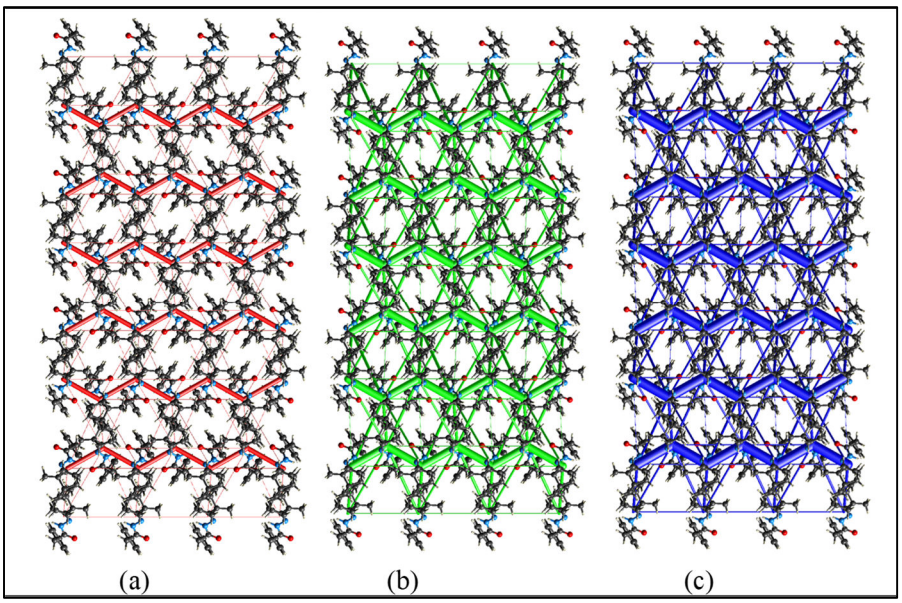

Figure 7. The energy frameworks calculated for MBL-101 showing the (a) electrostatic potential energy, (b) dispersion energy, and (c) total energy. The energy frameworks were adjusted to the same scale factor of tube size 80 with a cut-off value of 0.5 kJ mole $^{-1}$ within 3 × 3 × 3 unit cells and energy theory B3LYP/6-31G(d,p).

Interaction energies are calculated for a 3.8 Å cluster around the selected fragments. The interaction energy analysis for MBL-101, calculated using the B3LYP/6-31G(d,p) level of theory, reveals a range of intermolecular interactions characterized by varying symmetries and distances. The closest significant interaction occurs at a distance of 4.39 Å (symmetry operation: x+1/2,−y+1/2,zx+1/2, -y+1/2, z), where the total interaction energy (E_{tot}) is -72.4 kJ/mol. This interaction is dominated by a strong dispersion component (E_{dis}= -63.6 kJ/mol) and significant electrostatic (E_{ele}= -31.6 kJ/mol) and polarization (E_{pol}= -12.8 kJ/mol) contributions, partially offset by a repulsion energy (E_{rep}= 41.8 kJ/mol). Other notable interactions include those at 8.22 Å and 8.90 Å, with total energies of -7.5 and -20.3 kJ/mol, respectively. These interactions are also largely driven by dispersion forces. At 11.01 Å (symmetry: −x+1/2,y+1/2,z+1/2-x+1/2, y+1/2, z+1/2), the interaction energy is -13.9 kJ/mol, where dispersion remains the major contributor. A similar symmetry appears at 10.69 Å with a slightly stronger interaction of -17.6 kJ/mol.

Longer-range contacts, such as those at 12.56 Å and 13.30 Å, exhibit weaker interactions, with E_{tot} ranging from -3.4 to -7.4 kJ/mol, again primarily due to dispersion. The weakest interaction observed is at 11.28 Å, with a total energy of -3.1 kJ/mol. Overall, the interaction landscape of MBL-101 is governed predominantly by dispersion energies, with varying contributions from electrostatic, polarization, and repulsive forces depending on the molecular orientation and distance. The scale factors applied to the benchmarked energy models using CE-B3LYP with B3LYP/6-31G(d,p) electron densities are as follows: the electrostatic energy component (k_{ele}) is scaled by a factor of 1.057, indicating a slight enhancement relative to the unscaled value. The polarization energy (k_{pol}) is scaled by 0.740, and the dispersion energy (k_{disp}) by 0.871, both reflecting moderate reductions. The repulsion energy (k_{rep}) is scaled by 0.618, indicating a more substantial decrease. These factors help improve the accuracy of interaction energy calculations by compensating for systematic over- or underestimation inherent to the computational method.

5. CRYSTAL DATA COLLECTION AND REFINEMENT

Data collection: APEX2 (Bruker, 2004) [5]; cell refinement: APEX2/SAINT (Bruker, 2004) [5]; data reduction: SAINT /XPREP (Bruker, 2004) [5]; structure solution: SIR92 (Altornare et al., 2014) [6]; structure refinement: SHELXL-97 (Sheldrick, 2008) [7]; molecular graphics: ORTEP-3 for Windows (Farrugia, 1997) [8] and Mercury (Bruno et al., 2002) [9]; software used to prepare material for publication: SHELXL-97 (Sheldrick, 2008) [7].

Geometry: All esds (except the esd in the dihedral angle between two l.s. planes) are estimated using the full covariance matrix. The cell esds are taken into account individually in the estimation of esds in distances, angles, and torsion angles; correlations between esds in cell parameters are only used when they are defined by crystal symmetry. An approximate (isotropic) treatment of cell esds is used for estimating esds involving l.s. planes.

CCDC no. 2290403 contains the supplementary crystallographic data for this paper. These data can be obtained free of charge from The Cambridge Crystallographic Data Centre via www.ccdc.cam.ac.uk/data_request/cif.

Acknowledgement

Authors are thankful to Department of Chemistry, H. &. H. B. Kotak institute of Science, Rajkot and Envitro Laboratories Pvt Ltd. For laboratory facility and also thankful to SXRD facility is provided by STIC-Cochin Sponsored Jointly by KSCSTE and CUSAT.

Table 1. Crystal data and structure refinement for title compound.

Empirical formula	$C_{18}\ H_{24}\ N_2\ O$
Formula weight	284.39
Temperature	296(2) K
Wavelength	0.71073 Å
Crystal system, space group	Orthorhombic, $Pna2_1$
Unit cell dimensions	a = 8.2157(5) Å alpha = 90 deg. b = 15.6570(13) Å beta = 90 deg. c = 12.5573(10) Å gamma = 90 deg.
Volume	1615.3(2) $Å^3$
Z, Calculated density	4, 1.169 Mg/m^3
Absorption coefficient	0.073 mm^{-1}
F(000)	616
Crystal size	0.600 x 0.500 x 0.400 mm
Theta range for data collection	2.800 to 28.419 deg.
Limiting indices	-10<=h<=9, -20<=k<=20, -16<=l<=16
Reflections collected / unique	18913 / 3798 [R(int) = 0.0402]
Completeness to theta = 25.242	99.7 %
Absorption correction	Semi-empirical from equivalents
Max. and min. transmission	0.971 and 0.958
Refinement method	Full-matrix least-squares on F^2
Reflection / restraints / parameters	3798 / 2 / 193
Goodness-of-fit on F^2	1.028
Final R indices [I>2sigma(I)]	R1 = 0.0582, wR2 = 0.1454
R indices (all data)	R1 = 0.0746, wR2 = 0.1578
Absolute structure parameter	-0.4(5)
Extinction coefficient	n/a
Largest diff. peak and hole	0.410 and -0.288 (e $Å^{-3}$)

Table 2. Data collection and Refinement.

Data collection	
Diffractometer	Bruker axs kappa apex2 CCD Diffractometer
Scan method	ω and ϕ scan
Absorption correction	Multi-scan *SADABS* V2012/1 (Bruker AXS Inc.)
T_{min}, T_{max}	0.958, 0.971
No. of measured, independent and observed [$I > 2\sigma(I)$] reflections	18913, 3798, 3073
R_{int}	0.040
θ values (°)	θ_{max} = 28.4, θ_{min} = 2.8
$(\sin \theta/\lambda)_{max}$ (Å^{-1})	0.670
Range of *h*, *k*, *l*	*h* = -10→9, *k* = -20→20, *l* = -16→16
Refinement	
Refinement on	F^2
$R[F^2 > 2\sigma(F^2)]$, $wR(F^2)$, *S*	0.058, 0.158, 1.03
No. of reflections	3798
No. of parameters	193
No. of restraints	2
H-atom treatment	H-atom parameters constrained
Weighting scheme	$w = 1/[\sigma^2(F_o^2) + (0.0767P)^2 + 0.6393P]$ where $P = (F_o^2 + 2F_c^2)/3$
$(\Delta/\sigma)_{max}$	0.007
$\Delta\rangle_{max}$, $\Delta\rangle_{min}$ (e Å^{-3})	0.41, -0.29
Absolute structure	Flack x determined using 1167 quotients [(I+)-(I-)]/[(I+)+(I-)] (Parsons, Flack and Wagner, Acta Cryst. B69 (2013) 249-259).
Absolute structure parameter	-0.4 (5)

Table 3. Atomic coordinates (x 10^4) and equivalent isotropic displacement parameters (Å^2 x 10^3) for MBL-101. U(eq) is defined as one third of the trace of the orthogonalized Uij tensor.

	x	y	z	U(eq)
C(1)	5295(5)	994(3)	2630(3)	48(1)
C(2)	5111(6)	1021(4)	1545(4)	66(1)
C(3)	5823(6)	1677(4)	964(3)	70(1)
C(4)	6708(7)	2268(4)	1471(4)	77(2)
C(5)	6928(5)	2245(3)	2566(4)	59(1)
C(6)	6228(4)	1598(2)	3151(3)	36(1)
C(7)	6502(4)	1543(2)	4336(3)	42(1)
C(8)	5141(4)	1950(2)	4975(2)	34(1)
C(9)	5036(4)	3495(2)	6954(3)	36(1)
C(10)	6739(4)	3834(3)	7106(3)	45(1)
C(11)	6540(5)	4377(3)	8099(4)	64(1)
C(12)	6285(7)	3721(4)	9065(4)	76(2)
C(13)	4648(7)	3394(3)	8880(4)	65(1)
C(14)	4001(5)	3873(3)	7827(3)	52(1)
C(15)	4848(5)	4736(3)	8007(4)	56(1)
C(16)	4231(6)	5224(4)	8988(4)	74(2)
C(17)	4685(9)	5311(3)	7016(4)	90(2)
C(18)	2192(5)	3813(3)	7671(4)	52(1)
N(1)	4483(3)	2955(2)	6293(2)	34(1)
N(2)	5611(3)	2598(2)	5604(2)	34(1)
O(1)	3747(3)	1687(2)	4923(2)	49(1)

Table 4. Geometric parameters, Bond lengths [Å] and angles [º deg] for MBL-101.

C(1)-C(2)	1.372(6)	C(8)-C(7)-H(7A)	109.0
C(1)-C(6)	1.381(5)	C(6)-C(7)-H(7B)	109.0
C(1)-H(1)	0.9300	C(8)-C(7)-H(7B)	109.0
C(2)-C(3)	1.389(7)	H(7A)-C(7)-H(7B)	107.8
C(2)-H(2)	0.9300	O(1)-C(8)-N(2)	123.9(3)
C(3)-C(4)	1.337(8)	O(1)-C(8)-C(7)	121.5(3)
C(3)-H(3)	0.9300	N(2)-C(8)-C(7)	114.6(3)
C(4)-C(5)	1.388(7)	N(1)-C(9)-C(14)	122.3(3)
C(4)-H(4)	0.9300	N(1)-C(9)-C(10)	130.5(3)
C(5)-C(6)	1.377(5)	C(14)-C(9)-C(10)	107.0(3)
C(5)-H(5)	0.9300	C(9)-C(10)-C(11)	101.6(3)
C(6)-C(7)	1.508(5)	C(9)-C(10)-H(10A)	111.4
C(7)-C(8)	1.517(4)	C(11)-C(10)-H(10A)	111.4
C(7)-H(7A)	0.9700	C(9)-C(10)-H(10B)	111.4
C(7)-H(7B)	0.9700	C(11)-C(10)-H(10B)	111.4
C(8)-O(1)	1.219(4)	H(10A)-C(10)-H(10B)	109.3
C(8)-N(2)	1.342(4)	C(15)-C(11)-C(10)	104.2(3)
C(9)-N(1)	1.269(4)	C(15)-C(11)-C(12)	100.2(4)
C(9)-C(14)	1.509(5)	C(10)-C(11)-C(12)	106.1(4)
C(9)-C(10)	1.508(5)	C(15)-C(11)-H(11)	114.9
C(10)-C(11)	1.517(5)	C(10)-C(11)-H(11)	114.9
C(10)-H(10A)	0.9700	C(12)-C(11)-H(11)	114.9
C(10)-H(10B)	0.9700	C(13)-C(12)-C(11)	103.0(4)
C(11)-C(15)	1.504(6)	C(13)-C(12)-H(12A)	111.2
C(11)-C(12)	1.603(8)	C(11)-C(12)-H(12A)	111.2
C(11)-H(11)	0.9800	C(13)-C(12)-H(12B)	111.2
C(12)-C(13)	1.458(8)	C(11)-C(12)-H(12B)	111.2
C(12)-H(12A)	0.9700	H(12A)-C(12)-H(12B)	109.1
C(12)-H(12B)	0.9700	C(12)-C(13)-C(14)	105.8(4)
C(13)-C(14)	1.610(7)	C(12)-C(13)-H(13A)	110.6

C(13)-H(13A)	0.9700	C(14)-C(13)-H(13A)	110.6
C(13)-H(13B)	0.9700	C(12)-C(13)-H(13B)	110.6
C(14)-C(18)	1.502(6)	C(14)-C(13)-H(13B)	110.6
C(14)-C(15)	1.537(6)	H(13A)-C(13)-H(13B)	108.7
C(15)-C(16)	1.535(6)	C(18)-C(14)-C(9)	116.0(3)
C(15)-C(17)	1.540(7)	C(18)-C(14)-C(15)	121.5(4)
C(16)-H(16A)	0.9600	C(9)-C(14)-C(15)	101.3(3)
C(16)-H(16B)	0.9600	C(18)-C(14)-C(13)	113.9(4)
C(16)-H(16C)	0.9600	C(9)-C(14)-C(13)	103.2(3)
C(17)-H(17A)	0.9600	C(15)-C(14)-C(13)	98.1(3)
C(17)-H(17B)	0.9600	C(11)-C(15)-C(16)	115.5(4)
C(17)-H(17C)	0.9600	C(11)-C(15)-C(14)	95.8(3)
C(18)-H(18A)	0.9600	C(16)-C(15)-C(14)	113.9(4)
C(18)-H(18B)	0.9600	C(11)-C(15)-C(17)	111.1(4)
C(18)-H(18C)	0.9600	C(16)-C(15)-C(17)	109.2(4)
N(1)-N(2)	1.385(3)	C(14)-C(15)-C(17)	110.8(4)
N(2)-H(2A)	0.8600	C(15)-C(16)-H(16A)	109.5
		C(15)-C(16)-H(16B)	109.5
C(2)-C(1)-C(6)	120.7(4)	H(16A)-C(16)-H(16B)	109.5
C(2)-C(1)-H(1)	119.7	C(15)-C(16)-H(16C)	109.5
C(6)-C(1)-H(1)	119.7	H(16A)-C(16)-H(16C)	109.5
C(1)-C(2)-C(3)	119.8(5)	H(16B)-C(16)-H(16C)	109.5
C(1)-C(2)-H(2)	120.1	C(15)-C(17)-H(17A)	109.5
C(3)-C(2)-H(2)	120.1	C(15)-C(17)-H(17B)	109.5
C(4)-C(3)-C(2)	119.4(4)	H(17A)-C(17)-H(17B)	109.5
C(4)-C(3)-H(3)	120.3	C(15)-C(17)-H(17C)	109.5
C(2)-C(3)-H(3)	120.3	H(17A)-C(17)-H(17C)	109.5
C(3)-C(4)-C(5)	121.6(5)	H(17B)-C(17)-H(17C)	109.5
C(3)-C(4)-H(4)	119.2	C(14)-C(18)-H(18A)	109.5
C(5)-C(4)-H(4)	119.2	C(14)-C(18)-H(18B)	109.5
C(6)-C(5)-C(4)	119.5(4)	H(18A)-C(18)-H(18B)	109.5
C(6)-C(5)-H(5)	120.2	C(14)-C(18)-H(18C)	109.5

C(4)-C(5)-H(5)	120.2	H(18A)-C(18)-H(18C)	109.5
C(5)-C(6)-C(1)	118.9(3)	H(18B)-C(18)-H(18C)	109.5
C(5)-C(6)-C(7)	120.4(3)	C(9)-N(1)-N(2)	115.9(3)
C(1)-C(6)-C(7)	120.7(3)	C(8)-N(2)-N(1)	118.7(3)
C(6)-C(7)-C(8)	112.8(3)	C(8)-N(2)-H(2A)	120.7
C(6)-C(7)-H(7A)	109.0	N(1)-N(2)-H(2A)	120.7

Table 5. Anisotropic displacement parameters ($Å^2$ x 10^3) for MBL-101
The anisotropic displacement factor exponent takes the form:
-2 pi^2 [h^2 a*^2 U11 + ... + 2 h k a* b* U12].

	U^{11}	U^{22}	U^{33}	U^{23}	U^{13}	U^{12}
C(1)	47(2)	53(2)	44(2)	-4(2)	3(2)	-5(2)
C(2)	60(3)	84(3)	54(2)	-16(2)	-6(2)	-6(2)
C(3)	68(3)	108(4)	36(2)	4(2)	4(2)	14(3)
C(4)	79(3)	80(3)	72(3)	27(3)	11(3)	-6(3)
C(5)	56(2)	56(2)	64(3)	1(2)	4(2)	-12(2)
C(6)	29(2)	40(2)	39(2)	-7(1)	7(1)	9(1)
C(7)	34(2)	53(2)	40(2)	-14(2)	0(1)	12(2)
C(8)	30(2)	40(2)	31(2)	-5(1)	2(1)	3(1)
C(9)	31(2)	40(2)	37(2)	-5(1)	7(1)	-1(1)
C(10)	35(2)	53(2)	48(2)	-15(2)	3(2)	-8(2)
C(11)	52(2)	70(3)	70(3)	-34(2)	-1(2)	-14(2)
C(12)	95(4)	87(4)	44(2)	-5(2)	-13(2)	31(3)
C(13)	85(3)	63(3)	47(2)	11(2)	19(2)	16(2)
C(14)	47(2)	55(2)	55(2)	-22(2)	12(2)	-2(2)
C(15)	55(2)	53(2)	59(2)	-20(2)	-3(2)	4(2)

C(16)	73(3)	76(3)	72(3)	-44(3)	-10(2)	14(2)
C(17)	164(6)	48(2)	57(3)	14(2)	18(3)	39(3)
C(18)	43(2)	55(2)	57(2)	-16(2)	14(2)	2(2)
N(1)	28(1)	37(1)	38(1)	-9(1)	7(1)	1(1)
N(2)	22(1)	45(2)	36(1)	-9(1)	2(1)	0(1)
O(1)	32(1)	63(2)	53(2)	-23(1)	4(1)	-7(1)

Table 6. Hydrogen coordinates (x 10^4) and isotropic displacement parameters (Å^2 x 10^3) for MBL-101.

	x	y	z	U(eq)
H(1)	4787	565	3020	58
H(2)	4511	601	1199	79
H(3)	5686	1705	230	84
H(4)	7188	2705	1079	92
H(5)	7544	2664	2903	70
H(7A)	7521	1823	4511	51
H(7B)	6599	947	4538	51
H(10A)	7084	4176	6502	55
H(10B)	7513	3375	7219	55
H(11)	7397	4802	8210	77
H(12A)	7084	3265	9043	91
H(12B)	6357	4010	9747	91
H(13A)	3949	3517	9482	78
H(13B)	4672	2780	8770	78
H(16A)	4045	4829	9560	110
H(16B)	3232	5510	8815	110
H(16C)	5030	5637	9202	110
H(17A)	5252	5838	7137	134

H(17B)	3556	5426	6885	134
H(17C)	5147	5025	6411	134
H(18A)	1890	4117	7037	77
H(18B)	1647	4059	8273	77
H(18C)	1883	3224	7601	77
H(2A)	6593	2788	5580	41

Table 7. Torsion angles [º deg] for MBL-101.

C(6)-C(1)-C(2)-C(3)	-2.2(7)	C(10)-C(9)-C(14)-C(13)	-70.4(4)
C(1)-C(2)-C(3)-C(4)	1.3(8)	C(12)-C(13)-C(14)-C(18)	-163.9(4)
C(2)-C(3)-C(4)-C(5)	-0.3(8)	C(12)-C(13)-C(14)-C(9)	69.5(4)
C(3)-C(4)-C(5)-C(6)	0.3(8)	C(12)-C(13)-C(14)-C(15)	-34.2(4)
C(4)-C(5)-C(6)-C(1)	-1.2(6)	C(10)-C(11)-C(15)-C(16)	172.3(4)
C(4)-C(5)-C(6)-C(7)	177.7(4)	C(12)-C(11)-C(15)-C(16)	62.7(5)
C(2)-C(1)-C(6)-C(5)	2.1(6)	C(10)-C(11)-C(15)-C(14)	52.4(4)
C(2)-C(1)-C(6)-C(7)	-176.8(4)	C(12)-C(11)-C(15)-C(14)	-57.3(4)
C(5)-C(6)-C(7)-C(8)	96.1(4)	C(10)-C(11)-C(15)-C(17)	-62.6(5)
C(1)-C(6)-C(7)-C(8)	-85.0(4)	C(12)-C(11)-C(15)-C(17)	-172.3(4)
C(6)-C(7)-C(8)-O(1)	61.4(5)	C(18)-C(14)-C(15)-C(11)	-179.9(4)
C(6)-C(7)-C(8)-N(2)	-120.0(3)	C(9)-C(14)-C(15)-C(11)	-49.7(4)
N(1)-C(9)-C(10)-C(11)	-174.2(4)	C(13)-C(14)-C(15)-C(11)	55.6(4)
C(14)-C(9)-C(10)-C(11)	1.3(4)	C(18)-C(14)-C(15)-C(16)	58.9(5)
C(9)-C(10)-C(11)-C(15)	-34.3(4)	C(9)-C(14)-C(15)-C(16)	-170.8(4)
C(9)-C(10)-C(11)-C(12)	71.0(4)	C(13)-C(14)-C(15)-C(16)	-65.6(4)
C(15)-C(11)-C(12)-C(13)	36.3(4)	C(18)-C(14)-C(15)-C(17)	-64.7(5)

C(10)-C(11)-C(12)-C(13)	-71.9(4)	C(9)-C(14)-C(15)-C(17)	65.6(4)
C(11)-C(12)-C(13)-C(14)	-0.6(4)	C(13)-C(14)-C(15)-C(17)	170.8(4)
N(1)-C(9)-C(14)-C(18)	-19.6(6)	C(14)-C(9)-N(1)-N(2)	-173.6(3)
C(10)-C(9)-C(14)-C(18)	164.4(4)	C(10)-C(9)-N(1)-N(2)	1.3(6)
N(1)-C(9)-C(14)-C(15)	-153.2(4)	O(1)-C(8)-N(2)-N(1)	4.7(5)
C(10)-C(9)-C(14)-C(15)	30.8(4)	C(7)-C(8)-N(2)-N(1)	-173.9(3)
N(1)-C(9)-C(14)-C(13)	105.6(4)	C(9)-N(1)-N(2)-C(8)	172.2(3)

Table 8. Surface Property Information.

Name	Min	Mean	Max	Units
d i	0.820	1.634	2.557	Å
d e	0.821	1.650	2.458	Å
d norm	-0.484	0.579	1.527	
Shape Index	-0.995	0.244	0.998	
Curvedness	-3.970	-0.957	0.325	

Table 9. General Surface Information.

Type	Hirshfeld
Resolution	High (Standard)
Isovalue	0.5
Volume	396.54 Å³
Area	354.29 Å²
Globularity	0.737
Asphericity	0.302

Table 10. Supplementary Surface Property Statistics.

Name	Mean+	Mean-	Pi	Sigma+	Sigma-	SigmaT	Nu
d i	1.63	~	0.219	6.13E+09	~	2.94E+14	0
d e	1.65	~	0.222	6.25E+09	~	3.00E+14	0
d norm	0.592	-0.176	0.226	7.76E+08	2.08E+04	3.66E+13	4.64E-07
Shape Index	0.554	-0.459	0.448	3.39E+08	4.51E+07	1.19E+13	0.0523
Curvedness	0.0648	-0.968	0.426	981	2.11E+09	9.99E+13	4.75E-09

Table 11. Fingerprint Breakdown (Filtering fingerprint by element type).

Inside Atom	Outside Atom C	H	N	O	
C	.	7.9	.	.	7.9
H	6.2	69.2	3	4.7	83.1
N	.	3.6	.	.	3.6
O	.	5.3	.	.	5.3
	6.2	86.1	3	4.7	

Table 12. Interaction energy details for MBL-101.

N	Symop	R	Electron Density	E_ele	E_pol	E_dis	E_rep	E_tot
2	-x+1/2, y+1/2, z+1/2	11.01	B3LYP/6-31G(d,p)	-2.0	-1.7	-17.3	7.3	-13.9
2	x, y, z	8.22	B3LYP/6-31G(d,p)	-2.6	-0.5	-5.1	0.1	-7.5
2	x+1/2, -y+1/2, z	4.39	B3LYP/6-31G(d,p)	-31.6	-12.8	-63.6	41.8	-72.4
2	-x, -y, z+1/2	11.28	B3LYP/6-31G(d,p)	-0.1	-0.2	-3.2	0.1	-3.1
2	-x+1/2, y+1/2, z+1/2	10.69	B3LYP/6-31G(d,p)	-1.8	-0.5	-24.5	9.7	-17.6
2	x, y, z	12.56	B3LYP/6-31G(d,p)	-0.3	-0.1	-11.1	4.6	-7.2
2	x+1/2, -y+1/2, z	13.30	B3LYP/6-31G(d,p)	0.0	-0.1	-4.1	0.3	-3.4
2	x+1/2, -y+1/2, z	13.30	B3LYP/6-31G(d,p)	-0.5	-0.1	-9.4	2.3	-7.4
2	-x, -y, z+1/2	8.90	B3LYP/6-31G(d,p)	-2.4	-0.8	-24.8	7.1	-20.3

Table 13. Scale factors for benchmarked energy models.

Energy Model	k_ele	k_pol	k_disp	k_rep
CE-B3LYP ... B3LYP/6-31G(d,p) electron densities	1.057	0.740	0.871	0.618

References

[1] M. K. Vara, M. B. Parmar, M. Modak, J. H. Pandya. Substituted Camphor-Hydrazide Schiff Bases: Synthesis, Characterization, and Anticancer Activity. World Scientific News 2025;206:17-29.

[2] P. R. Spackman, M. J. Turner, J. J. McKinnon, S. K. Wolff, D. J. Grimwood, D. Jayatilaka, M. A. Spackman. CrystalExplorer: a program for Hirshfeld surface analysis, visualization and qu-antitative analysis of molecular crystals. J. Appl. Cryst. 2021;54(3):1006-11. https://doi.org/10.1107/S1600576721002910

[3] M. A. Spackman, J. J. McKinnon, Fingerprinting Intermolecular Interactions in Molecular Crystals. CrystEngComm. 2002;4(66):378-92. https://doi.org/10.1039/B203191B

[4] J. J. McKinnon, D. Jayatilaka, M. A. Spackman, Towards quantitative analysis of intermolecular interactions with Hirshfeld surfaces. Chem Commun. 2007;(37):3814-6. https://doi.org/10.1039/B704980C

[5] Bruker. APEX2 and SAINT. Bruker AXS Inc. 2004 Madison, Wisconsin, USA.

[6] Altornare, G. Cascarano, C. Giacovazzo, A. J. Guagliardi. SIR92, Appl. Cryst. 1993;26:343-50. https://doi.org/10.1107/S0021889892010331

[7] G. M. Sheldrick. short history of SHELX. Acta Cryst. 2008;A64:112-22. https://doi.org/10.1107/S0108767307043930

[8] L. J. Farrugia. WinGX and ORTEP for Windows: an update. J. Appl. Cryst. 2012;45:849-54. https://doi.org/10.1107/S0021889812029111

[9] J. Bruno, J. C. Cole, P. R. Edgington, M. Kessler, C. F. Macrae, P. McCabe, J. Pearson, R. Taylor. New software for searching the Cambridge Structural Database and visualizing crystal structures. Acta Cryst. (2002). B58, 389-97. https://doi.org/10.1107/S0108768102003324